Journal of Vasyl Stefanyk Precarpathian National University. Biology
V.12 (2025) pp. 46-59

Vasyl Stefanyk Carpathian National University

DOI: 10.15330/jpnubio.12.46-59

ISSN(Online): 3083-662X
ISSN(Print): 3083-6611

UDC: 595.76:577.21:575.17

Molecular Cross-Validation of Intraspecific Structure of *Rutpela maculata* (Insecta: Coleoptera: Cerambycidae)

Andrew Zamoroka[1*], Oleksandr Zinenko[2]

[1] *Laboratory of Animal Phylogeny and Evolution, Department of Biology and Ecology, Vasyl Stefanyk Carpathian National University*
[2] *The Museum of Nature, and Department of Zoology and Animal Ecology, School of Biology, V. N. Karazin Kharkiv National University*

*Corresponding author: Andrew Zamoroka: andrii.zamoroka@cnu.edu.ua

Received: 23 November 2025; **Revised:** 08 December 2025; **Accepted:** 14 December 2025; **Published:** 15 December 2025

Abstract

Rutpela (Rutpela) maculata (Poda, 1761) is one of the most abundant and widespread lepturine beetles in Europe, ranging from the Atlantic coast to the southern Ural Mountains. The intraspecific taxonomy of *R. maculata* has been debated for decades, with no consensus on subdivision based on morphological traits. Here, we conducted a phylogenetic analysis of the species' intraspecific structure using newly generated DNA barcodes from Croatia, Italy, Slovenia, Spain, and Ukraine, combined with sequences from public databases (GenBank, BOLD Systems, CaBOL). Our results reveal three distinct haplogroups (*weRM*, *ceRM*, *esRM*) within the species' range, each clearly associated with morphological patterns, particularly limb and antennae melanization in males. The melanistic forms corresponding to the *weRM* haplogroup in southwestern Europe and the *esRM* haplogroup in the Caucasus-Anatolian region arose independently from different ancestors. In contrast, the *ceRM* haplogroup is broadly distributed across Europe, from Finland and Norway to Italy, Greece and Türkiye. Two of three studied haplogroups correspond to previously recognized subspecies, *R. m. maculata* (*ceRM*) and *R. m. manca* (*weRM*). The third haplogroup, *esRM*, previously considered part of *R. m. manca*, represents a separate evolutionary lineage, distantly related to *ceRM*, and is here formally recognized as a new subspecies, *Rutpela maculata orientalis* **ssp. nov**. Genetic distances, COI sequence divergences, morphological differentiation, and geographic separation collectively support this taxonomic revision. Our study demonstrates the effectiveness of molecular phylogenetic approaches in resolving the long-standing issues of intraspecific classification and geographic delineation of *R. maculata* subtaxa.

Keywords: longhorn beetles, molecular phylogeny, molecular phylogeography, taxonomy, PCR, DNA barcoding

1. INTRODUCTION

Rutpela (Rutpela) maculata (Poda, 1761) is one of the most abundant and widespread lepturine beetles in Europe (Vitali 2018). The species is broadly distributed across the continent, from the Atlantic coast in the west to the southern Ural Mountains in the east (Löbl & Smetana 2010). In northern Europe, the range of *R. maculata* reaches the southern Fennoscandian region, although isolated records occur north of 60° N. In the south, the species inhabits mountain systems of the northern Mediterranean, occurring sporadically from the Iberian Peninsula to the Middle East (Löbl & Smetana 2010; Vitali 2018). *R. maculata* is also common in the Caucasus and the Crimean Mountains. Due to the dominance of steppe landscapes in the northern Black Sea region, the distribution range of *R. maculata* is disrupted (Zamoroka 2022a), separating its Eastern European and Crimean-Caucasian populations.

Rutpela maculata is a highly polymorphic species, exhibiting extensive morphological variation throughout its range. The number, shape, and size of black spots on the elytra vary considerably, as does the degree of pigmentation in the legs and antennal segments (Danilevsky 2015). Mediterranean populations are generally more melanistic compared to those of Central and Eastern Europe (Danilevsky 2015; Vitali 2018). Such variability has historically led to multiple redundant descriptions of the species under different names. During the 19th and 20th centuries, more than thirty color forms of *R. maculata* were described (Mulsant 1839; Pic 1933, 1937, 1945; Heyrovský 1936; Podaný 1963), underscoring the pronounced variability of the species, which is rooted in polyallelism.

Over the last two decades, the intraspecific taxonomy of *R. maculata* has been a subject of active debate (Rapuzzi & Sama 2006; Löbl & Smetana 2010; Özdikmen et al. 2012; Danilevsky 2015). At present, no consensus has been reached regarding its intraspecific subdivision based on morphological traits (Vitali 2018). Some authors recognize two subspecies (Danilevsky 2015), others three (Özdikmen et al. 2012), and still others four (Löbl & Smetana 2010). In sum, four subspecies are currently distinguished morphologically: *R. m. maculata* (Poda, 1761), *R. m. manca* (Schaufuss, 1863), *R. m. nigricornis* (Stierlin, 1864), and *R. m. irmasanica* Sama, 1996.

To date, the complete nuclear and mitochondrial genomes of *R. maculata* have been fully sequenced (Sivell et al. 2023). In addition, numerous DNA barcodes from across the species' range are available in public repositories such as GenBank, BOLD Systems, and CaBOL. However, no phylogeographic or taxonomic studies of the intraspecific structure of *R. maculata* using molecular methods have yet been conducted. It should be noted, nevertheless, that the phylogenetic relationships of *R. maculata* with its closest relatives and its placement within the tribe Lepturini are well established (Semaniuk & Zamoroka 2020; Zamoroka et al. 2022; Zamoroka 2022b).

In this study, we conducted a phylogenetic analysis of the intraspecific structure of *R. maculata* based on a synthesis of newly generated DNA barcodes from Croatia, Italy, Slovenia, Spain, and Ukraine, together with sequences available in public repositories (GenBank, BOLD Systems, CaBOL). Our results provide clear evidence for the existence of three major genetic lineages (haplogroups) within the range of *R. maculata*, corresponding to the well-known subspecies *R. m. maculata* and *R. m. manca* and a newly described here *R. m. orientalis* **ssp. nov**.

2. MATERIALS AND METHODS

Sample collections. During fieldwork from 2018 to 2023 in Croatia, Italy, Slovenia, Spain, and Ukraine, we collected adult specimens of *R. maculata* for sequencing. Each was preserved on site in 96% ethanol, carefully labeled, and transported to the laboratory, where the material was kept in ethanol at –20°C prior to DNA extraction.

DNA extraction. The muscles from the hind leg were used for DNA extraction and placed in individual wells of a 96-well PCR plate. Each well received 25 μL of lysis buffer C containing 200 mM Tris (pH 8.0), 25 mM EDTA (pH 8.0), 0.05% Tween-20, and 0.4 mg mL^{-1} Proteinase K (Korlević

et al. 2021). The tissue was homogenized to ensure uniform distribution of the buffer and then incubated at 56°C for 2 h to promote complete cell lysis and DNA release. Following incubation, a 10-fold dilution of the lysate was prepared, and all subsequent PCR reactions were performed directly on the unpurified DNA solution, thereby reducing processing time and reagent use (Korlević et al. 2021; Makunin et al. 2022).

PCR. Indexed universal COI primers HCO and LCO were used for PCR amplification (Srivathsan et al. 2021). Each 10 μL reaction consisted of 5 μL of Master Mix (MM), 0.3 μL of forward primer (Pr F), 0.3 μL of reverse primer (Pr R), 3.2 μL of distilled water, 0.7 μL of DNA template, and 0.5 μL of dimethyl sulfoxide (DMSO). The components were gently mixed in thin-walled PCR tubes to avoid introducing bubbles. PCR cycling began with an initial denaturation at 95°C for 2 min, followed by 25–35 cycles of 95°C for 30 s (denaturation), 40°C for 30 s (annealing), and 72°C for 45 s (extension). A final extension step at 72°C for 5 min completed the amplification. Two microlitres of each PCR product were immediately analyzed by gel electrophoresis to confirm successful amplification, and the remaining volume was stored at 4 °C for subsequent sequencing.

Library preparation and Sequencing. The Oxford Nanopore Technologies (ONT) DNA-barcoding workflow described by Srivathsan et al. (2021) was followed. Briefly, PCR products carrying unique index combinations were pooled, purified, and prepared according to the standard ONT library preparation protocol, then sequenced on a MinION flow cell. Base calling was performed with ONT's software, and subsequent bioinformatic processing – including demultiplexing and consensus sequence generation – was carried out using ONTbarcoder 2.0 (Srivathsan et al. 2024).

Phylogenetic analysis. Phylogenetic analyses were performed in Seaview 5.0, a cross-platform tool for multiple sequence alignment, molecular phylogenetics, and tree reconciliation (Gouy et al. 2021). Sequence alignments were generated with the integrated MUSCLE algorithm and then inspected and manually adjusted to remove ambiguous or poorly aligned regions. Maximum-likelihood trees were inferred using the PhyML module (Guindon et al. 2010) under the general time-reversible (GTR) substitution model. Branch support was evaluated with the approximate likelihood-ratio test (aLRT), which compares the likelihood of the current topology to that of the best alternative (Anisimova & Gascuel 2006; Guindon et al. 2010). Tree optimization combined nearest-neighbor interchange (NNI) with subtree pruning and regrafting (SPR), and branch lengths were further refined using the neighbor-joining-based BioNJ algorithm (Gascuel 1997). In total seventy-seven DNA barcode sequences (Table 1) were involved into the final phylogenetic analysis.

Table 1. Geographic and repository data for *Rutpela maculata* DNA barcode vouchers, used in this study

Voucher number	Repository	Country of origin	Geographical coordinates
CaBOL-1027328	CaBOL	Georgia, Shida Kartli	41.959777, 44.158741
CaBOL-1027329	CaBOL	Georgia, Shida Kartli	41.979584, 44.120380
CaBOL-1027330	CaBOL	Georgia, Shida Kartli	41.907896, 44.090114
CERLF230-08	BOLDsys	France, Normandie	49.583, -1.729
COLAT173-08	BOLDsys	Switzerland, Develier	47.362, 7.293
COLAT174-08	BOLDsys	Switzerland, Develier	47.362, 7.293
COLAT175-08	BOLDsys	Switzerland, Develier	47.362, 7.293
COLFE667-13	BOLDsys	Sweden, Borgholm	56.768, 16.618
COLFG040-13	BOLDsys	Finland, Savonia australis	61.4866, 28.2294
COLHH1533-18	BOLDsys	Norway, Rogaland	59.4486, 6.02121
DTNHM4488-22	BOLDsys	United Kingdom, Hartslock	51.5118, -1.113592
DTNHM5193-23	BOLDsys	United Kingdom, England	51.188206, 0.117129

DTNHM7504-23	BOLDsys	United Kingdom, Norfolk	52.6925, 1.4594
DTNHM8527-23	BOLDsys	United Kingdom, Norfolk	52.6925, 1.4594
FBCOB363-10	BOLDsys	Germany, Rhineland-Palatinate	50.317825, 7.494663
FBCOC130-10	BOLDsys	Germany, Bavaria	48.5649, 10.9093
GBCOB238-12	BOLDsys	Germany, North Rhine-Westphalia	51.66939, 6.806088
GBCOD464-13	BOLDsys	Germany, Rhineland-Palatinate	50.5243, 7.037164
GBCOF652-13	BOLDsys	Germany, North Rhine-Westphalia	50.764, 6.819
GBCOL353-12	BOLDsys	Slovenia, Obalno-kraka	45.5233, 13.5824
GBCOU5696-14	BOLDsys	Germany, Bavaria	47.554, 12.978
GBCOU609-13	BOLDsys	Germany, Rhineland-Palatinate	49.816967, 7.835542
GBMIX1723-15	BOLDsys	France, Normandie	48.586, -0.111
GBMIX1752-15	BOLDsys	France, Normandie	48.586, -0.111
GCOL1097-16	BOLDsys	Germany, North Rhine-Westphalia	50.6667, 7.2333
GCOL1146-16	BOLDsys	Germany, Thuringia	50.8622, 11.2975
GCOL1326-16	BOLDsys	Germany, North Rhine-Westphalia	50.6551, 7.05682
GCOL1334-16	BOLDsys	Germany, North Rhine-Westphalia	50.6455, 7.08126
GCOL4134-16	BOLDsys	Germany, Saxony	50.4366, 12.0707
GCOL4397-16	BOLDsys	Germany, Saxony-Anhalt	51.6735, 11.1918
GCOL4422-16	BOLDsys	Germany, Saxony Klosterbuch/Mulde	51.1495, 12.9837
GCOL4423-16	BOLDsys	Germany, Saxony Klosterbuch/Mulde	51.1495, 12.9837
GCOL463-16	BOLDsys	Germany, Thuringia	51.3096, 11.2552
GCOL506-16	BOLDsys	Germany, Thuringia	50.8612, 11.1268
GCOL540-16	BOLDsys	Germany, Thuringia	50.9366, 11.0132
GCOL599-16	BOLDsys	Germany, Rhineland-Palatinate	50.3179, 7.4946
GCOL609-16	BOLDsys	Germany, Rhineland-Palatinate	50.3179, 7.4946
GCOL782-16	BOLDsys	Germany, North Rhine-Westphalia	50.6667, 7.05
GMGMK020-14	BOLDsys	Germany, Rhineland-Palatinate	50.5557, 7.16988
GMGMK021-14	BOLDsys	Germany, Rhineland-Palatinate	50.5557, 7.16988
GMGMK022-14	BOLDsys	Germany, Rhineland-Palatinate	50.5557, 7.16988
GMGMK023-14	BOLDsys	Germany, Rhineland-Palatinate	50.5557, 7.16988
GMGMK024-14	BOLDsys	Germany, Rhineland-Palatinate	50.5557, 7.16988
GMGMK025-14	BOLDsys	Germany, Rhineland-Palatinate	50.5557, 7.16988
GMGMK026-14	BOLDsys	Germany, Rhineland-Palatinate	50.5557, 7.16988
GMGMK027-14	BOLDsys	Germany, Rhineland-Palatinate	50.5557, 7.16988
GMGMK029-14	BOLDsys	Germany, Rhineland-Palatinate	50.5557, 7.16988
GMGML285-14	BOLDsys	Germany, Rhineland-Palatinate	50.5557, 7.16988
GMGML286-14	BOLDsys	Germany, Rhineland-Palatinate	50.5557, 7.16988
GMGMM291-14	BOLDsys	Germany, Rhineland-Palatinate	50.5557, 7.16988
HMYZ267-23	BOLDsys	Slovakia, Bratislava	48.233335, 17.167133
ICRYO038-22	BOLDsys	Croatia, Bjelovar-Bilogora	46.013, 16.921
LPRCC189-19	BOLDsys	France, Corsica	42.49389, 8.992727
LPRCC714-21	BOLDsys	France, Corsica	41.773, 9.122
LPRCI2244-22	BOLDsys	France, Corsica	41.70565, 9.397549
LPRCI2245-22	BOLDsys	France, Corsica	41.53017, 9.23211
LPRCI858-21	BOLDsys	France, Corsica	41.529, 9.231
NLCOB528-12	BOLDsys	Netherlands, Limburg	50.875, 5.765
NLCOB529-12	BOLDsys	Netherlands, Limburg	50.875, 5.765
NOCLP2027-20	BOLDsys	Norway, Ostfold	59.052, 10.95

NOCLP2028-20	BOLDsys	Norway, Vest-Agder	58.191, 8.07
POMS1152-24	BOLDsys	United Kingdom	51.507496, -1.0384105
PSFOR450-13	BOLDsys	France, Essonne	48.763, 2.242
PSFOR451-13	BOLDsys	France, Essonne	48.763, 2.242
PV658009*	GenBank	Ukraine, Ivano-Frankivska	49.322418, 24.664597
PX418918*	GenBank	Croatia, Lika-Senj	44.652605, 15.065594
PX418919*	GenBank	Italy, Pordenone	46.353529, 12.787459
PX418920*	GenBank	Slovenia, Central Slovenia	45.928220, 14.471913
PX418921*	GenBank	Spain, Barcelona	41.767862, 2.269963
TDAAT1099-20	BOLDsys	Austria, Lower Austria	48.184, 16.078
TDAAT1163-20	BOLDsys	Austria, Tyrol	47.551, 11.906
TDAAT933-20	BOLDsys	Austria, Lower Austria	48.202, 16.003
TDAOE3218-23	BOLDsys	Austria, Vienna	48.211666, 16.261667
TDAOE3347-23	BOLDsys	Austria, Carinthia	46.964558, 13.483744
ZFMK-TIS-8004030	CaBOL	Georgia, Racha-Lechkhumi and Kvemo Svaneti	42.700815, 42.841943
ZFMK-TIS-8013142	CaBOL	Armenia, Gegharkunik	40.700598, 45.120625
ZFMK-TIS-8013145	CaBOL	Armenia, Kajaran	39.249761, 46.111340

* Sequences obtained exclusively for this study

3. RESULTS AND DISCUSSION

As a result of our analyses, we obtained the most likelihood phylogenetic tree (Fig. 1A) resolving the intraspecific structure of *R. maculata*. All branches of the tree are strongly supported (SH ≥ 0.85). The topology indicates that *R. maculata* comprises two well-delineated genetic lineages, each represented by clades with very high support (SH = 0.94). Notably, the larger lineage exhibits clear signs of paraphyly, as it includes a long terminal subclade that is genetically distinct. We consider these three topological formations as separate haplogroups: 1) western (*weRM*); 2) central (*ceRM*); and 3) eastern (*esRM*) due to the geographical part of *R. maculata* range in the Western Palearctic. The mean COI sequence divergence between haplogroups is 3.8%, corresponding to approximately 20 nucleotide substitutions per sequence, with a minimum of 3.4% and a maximum of 4.2%. Pairwise genetic distances between haplogroups are: 1) *weRM* – *ceRM* = 0.015 substitutions per site; 2) *weRM* – *esRM* = 0.030 substitutions per site; 3) *ceRM* – *esRM* = 0.040 substitutions per site.

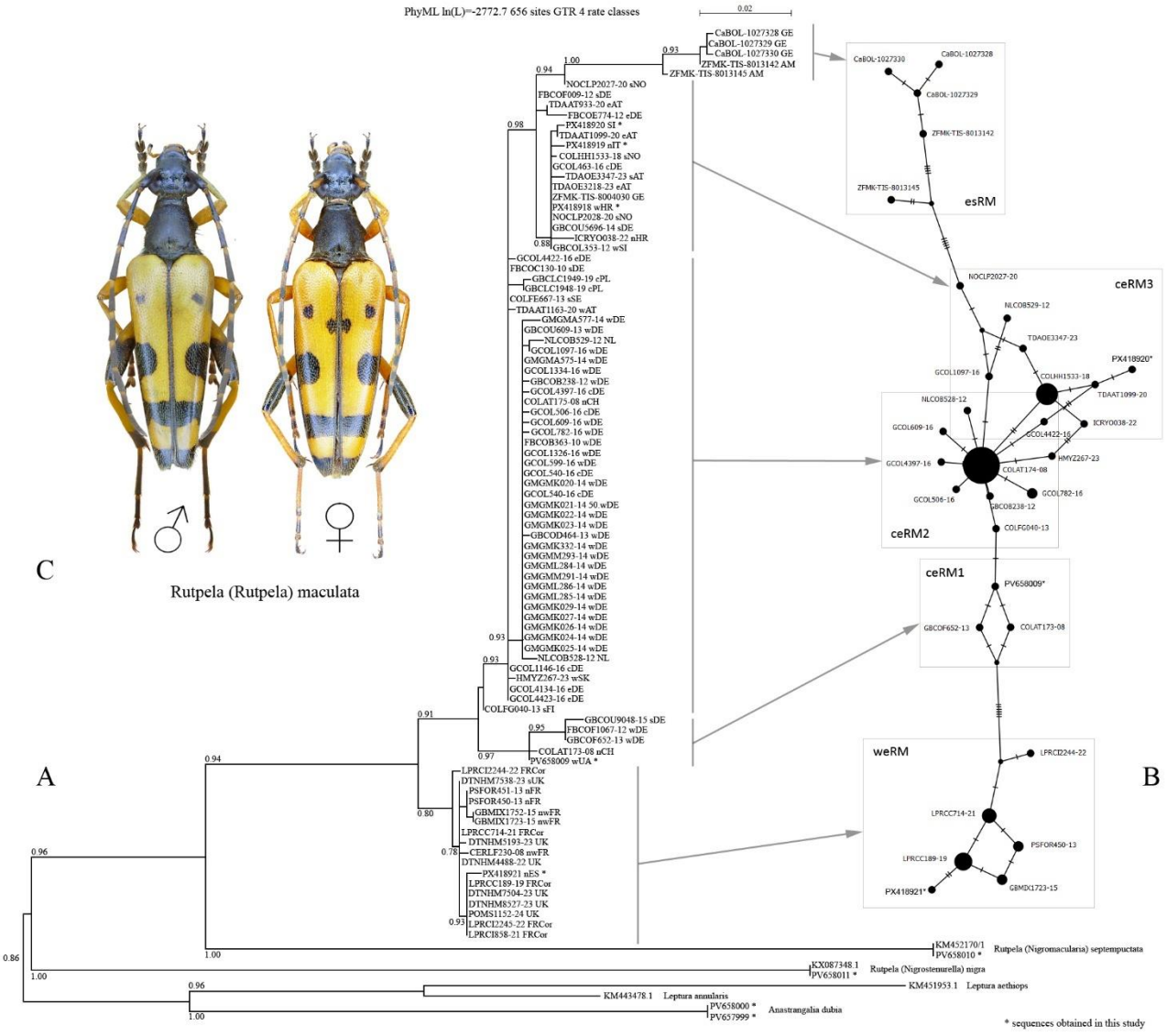

Figure 1. Intraspecies genetic diversity of *R. maculata*: (A) The maximum likelihood phylogenetic tree of *R. maculata*; (B) Network diagram illustrating intraspecies genetic distances within *R. maculata*; (C) General habitus of *R. maculata* collected in Ukraine (photo credit Zamoroka et al., 2022)

The *weRM* haplogroup comprises 17 barcoded specimens from Western Europe, including Spain, France (including Corsica), and the United Kingdom. COI sequences from these regions are highly homogeneous. The mean genetic distance among all specimens is 0.002 substitutions per site. The most divergent samples are from continental France (0.003 substitutions per site) and Spain (0.007 substitutions per site). Nevertheless, these genetic distances remain very low, indicating a shared origin for all populations within haplogroup *weRM*. Overall, sequence divergence among the analyzed specimens averages 0.4%, ranging from 0.0% to 0.8%, corresponding to approximately 2.8 nucleotide substitutions per sequence.

The *ceRM* haplogroup consists of 67 barcoded specimens with a broad geographic distribution across Europe, including Finland, Norway, the Netherlands, Germany, Poland, Ukraine, Slovakia, Austria, Switzerland, Italy, Slovenia, and Croatia. This haplogroup is not homogeneous and comprises three haplotypes: *ceRM1*, *ceRM2*, and *ceRM3*. The mean COI sequence divergence among haplotypes is 1.8%, ranging from 0.9% to 2.4%. Within haplotypes, the mean divergence between individual sequences is 0.2%, corresponding to one nucleotide substitution per sequence. No clear

geographic patterns of specific haplotypes were observed, as all are widely distributed across Europe. The mean genetic distance within the haplogroup is 0.013 substitutions per site.

Finally, the *esRM* haplogroup in our study is represented by five sequences originating from Georgia and Armenia. The mean genetic distance within the haplogroup is 0.010 substitutions per site. Notably, the sequence ZFMK-TIS-8004030 from Georgia clusters within the *ceRM3* haplotype, directly indicating waves of hybridization and migration from European populations into the Caucasus and likely into Anatolia.

Our results clearly demonstrate that multiple distinct genetic lineages, or haplogroups (*weRM*, *ceRM*, *esRM*), exist within the range of *R. maculata*, likely arising through divergent evolution following the fragmentation of the ancestral range. This pattern was probably driven by a series of Pleistocene glaciations, which caused "pulsations" in the species' distribution, with periods of range expansion during interstadials and contraction during stadials. Evidence supporting this scenario is provided by the complex network of relationships among haplotypes within the *ceRM* haplogroup, as illustrated in our network diagram (Fig. 1B).

The most geographically peripheral regions of the range, in southwestern Europe and the Caucasus-Anatolian region, also include the most genetically isolated populations, forming the *weRM* and *esRM* haplogroups, respectively. In contrast, the *ceRM* haplogroup is widespread across most of Europe and comprises at least three haplotypes: *ceRM1*, *ceRM2*, and *ceRM3*. These haplotypes form a complex reticulate genetic network. Moreover, all three haplotypes are intermixed within the same geographic area, indicating that they likely evolved independently in the past and were previously isolated from each other, with their current admixture occurring no later than the postglacial transition during the Holocene. Very similar results of haplotypes overlapping we demonstrated in the series of our recent studies on other European cerambycids (Zamoroka & Zinenko 2024; Zamoroka 2025a, b).

All three haplogroups are clearly associated with morphological patterns in *R. maculata*, particularly limb melanization, which is especially pronounced in males. Specifically, the *ceRM* haplogroup occurs almost exclusively in "light-legged" individuals, whereas the *weRM* and *esRM* haplogroups are associated with "dark-legged" individuals. Based on these morphological color patterns, *R. maculata* was divided into two main subspecies: *R. m. maculata* and *R. m. manca* (Özdikmen et al. 2012; Danilevsky 2015) The primary distinction between these subspecies is the pronounced melanization of the limbs (especially the hind legs) and antennae in males, with a lesser degree observed in females of *R. m. manca*.

In the southern part of the species' range, melanistic morphs are widespread and, in some cases, dominant (Danilevsky 2015). The degree of melanization can vary significantly not only across the range but even within a single population, such that similar color patterns often appear among distantly related populations (Vitali 2018). Vitali (2018) also notes that the distribution of *R. maculata* in Southern Europe is largely restricted to mountainous regions. This clearly indicates the presence of so-called "mountain melanism" especially in males. Studies in other insects indicate that increased melanization provides physiological benefits for males, but not for females (Haque et al. 2024; Kutama et al. 2024). Interestingly, one intermediate product of melanin synthesis in insects is dopamine (Sugumaran & Barek 2016; Barek et al. 2017) – a neurotransmitter involved in the sensation of pleasure. It can be hypothesized that the higher degree of melanization of males in southern populations of *R. maculata* results from sexual selection driven by higher dopamine levels in their bodies.

Our study revealed a sympatric distribution of the *ceRM3* haplotype and the *esRM* haplogroup in the Caucasus. We also find traits of hybridization between the *ceRM3* and *esRM* genetic lineages. Notably, individuals carrying the *ceRM3* haplotype in this region are morphologically indistinguishable from those of the *esRM* haplogroup and exhibit melanistic traits. This provides strong evidence for at least one migratory wave of *ceRM3* from Europe into the Caucasus-Anatolian region. The exact route of this migration remains unclear due to the absence of genetic data for *R.*

maculata populations in Türkiye. A clue to resolving this conundrum comes from Özdikmen et al. (2012), who reported the sympatric occurrence of the two morphosubspecies *R. m. maculata* and *R. m. manca* (*R. m. nigricornis* – in the original paper) in Türkiye, as well as from our previous faunistic studies, which demonstrated a "steppe hiatus" in the southern Ukrainian range of *R. maculata* (Zamoroka 2022a). Our current results indicate that the *ceRM1* haplotype, which is the most divergent from *ceRM2* and *ceRM3*, is widespread in the Ukrainian plains. This suggests that the most probable migration route of *ceRM3* into the Caucasus passed through Türkiye. Furthermore, Özdikmen et al. (2012) noted the broad geographic distribution of *R. m. maculata* in Anatolia, albeit at low population densities.

Özdikmen et al. (2012) rightly raised the question of sympatry among the color forms of *R. maculata* in Türkiye, suggesting the presence of three subspecies: *R. m. maculata*, *R. m. manca*, and *R. m. irmasanica*. However, Özdikmen (2021) ultimately reached an erroneous conclusion by proposing that *R. m. manca* should be treated as a distinct species. Our analysis demonstrates that COI sequence divergence between *R. maculata* haplogroups reaches only 3-4%, which is insufficient to justify species-level distinction but is fully adequate to recognize them as subspecies. Accordingly, we propose a formal nomenclatural act synonymizing *Rutpela manca* (Schaufuss, 1863) **syn. nov**. and restoring its subspecies status as *Rutpela maculata manca* (Schaufuss, 1863) **ssp. stat. res**.

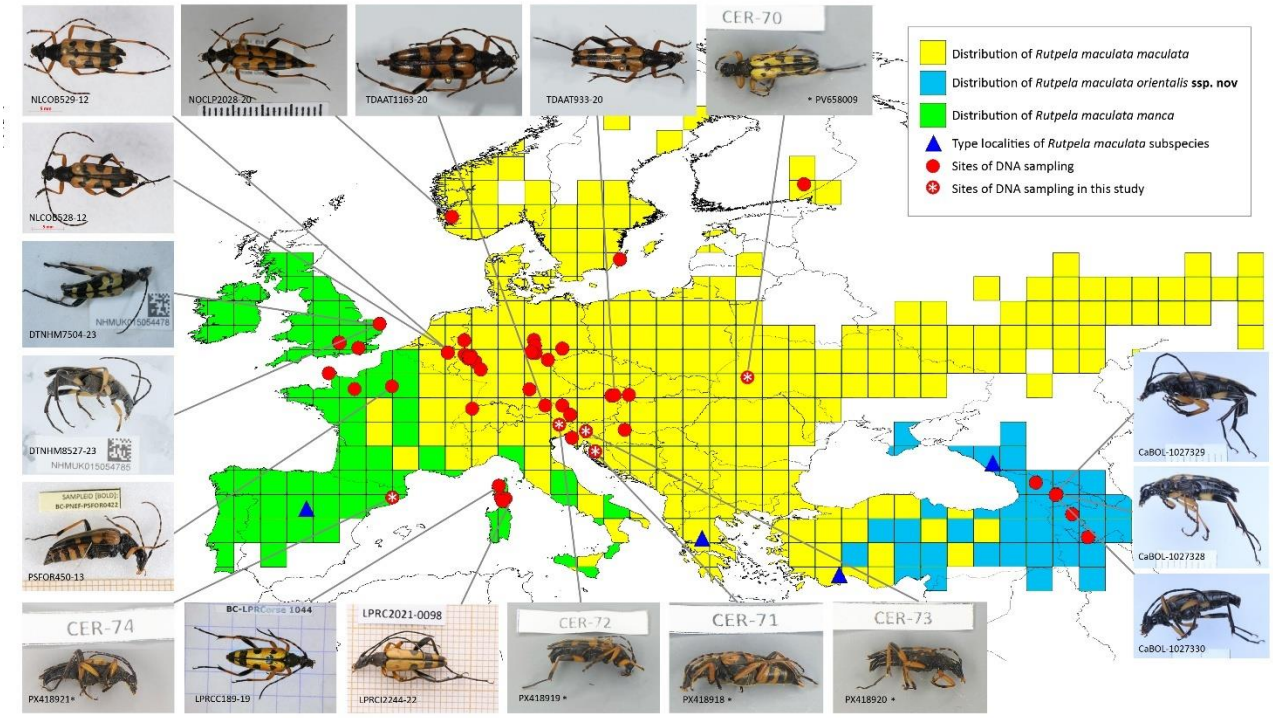

Figure 2. Geographic distribution of *Rutpela maculata* subspecies based on molecular and morphological data. Reference photographs from BOLD Systems and this study illustrate the color patterns of *Rutpela maculata* across its distribution range.

Furthermore, our results indicate that the melanistic forms corresponding to the *weRM* haplogroup in southwestern Europe and the *esRM* haplogroup in the Caucasus-Anatolian region arose independently from different ancestors. These melanistic forms do not form a continuous North Mediterranean range, which is instead disrupted in the northeastern Mediterranean (Fig. 2). In the Balkan Peninsula, "light-legged" morphs assigned to *R. m. maculata* are widespread. The type locality of the nominotypical subspecies *R. m. maculata* is in Greece (Poda 1761). On the Apennine Peninsula, both "light-legged" and "dark-legged" morphs occur sympatrically in the central and southern regions, while the northern regions are dominated by "light-legged" morphs. In France, both morphs also occur sympatrically, with "light-legged" forms predominating in the north and

east, and "dark-legged" forms in the south and west. A similar pattern occurs in Anatolia, where "light-legged" morphs are distributed in the western and central parts, and "dark-legged" morphs in the east (Özdikmen et al. 2012; Özdikmen 2021).

Regarding the subspecies *R. m. irmasanica*, the situation remains unclear, as only a few specimens are known from a very restricted area in Antalya, southern Türkiye, with males distinguished by a light-colored abdomen (all others have a dark abdomen) (Sama 1996; Özdikmen et al. 2012; Özdikmen 2021). The range of *R. m. irmasanica* is entirely nested within that of *R. m. maculata* (Özdikmen et al. 2012), where hybridization is possible. It is likely that these specimens represent merely color aberrations of highly demelanized individuals. Therefore, we cautiously suggest that *R. m. irmasanica* does not constitute a distinct subspecies. However, this question can be definitively resolved only after molecular analysis of either the type specimens described by Sama (1996) or specimens identical to them collected from the type locality.

Overall, our study demonstrates that at least three distinct genetic lineages, or haplogroups, of *R. maculata* exist in the Western Palaearctic. Two of these lineages correspond clearly to the recognized subspecies *R. m. maculata* (haplogroup *ceRM*) and *R. m. manca* (haplogroup *weRM*). The third haplogroup, *esRM*, was previously considered part of *R. m. manca.* However, our results show that it represents a distinct evolutionary lineage, somewhat related to the *ceRM* haplogroup, from which it likely evolved. Genetic distances and COI sequence divergences, together with morphological differences and geographic separation, provide strong justification for recognizing the *esRM* haplogroup as a new subspecies: *Rutpela maculata orientalis* **ssp. nov**.

Thus, molecular analyses allowed us to confirm the distinction of two morphosubspecies and to establish a new one, while one previously described morphosubspecies remains unassessed and may represent merely a color morph of some already existing subspecies. Based on the above presented results, we propose a new intraspecific classification of *R. maculata*:

Species: *Rutpela (Rutpela) maculata* (Poda, 1761)
Distribution: Western Palaearctic, excluding the extreme north and extreme south (Fig. 2).

Subspecies: *Rutpela (Rutpela) maculata maculata* (Poda, 1761)
Distribution: Europe, excluding the southwestern regions and the British Isles; Anatolia; ? Middle East (Fig. 2).

? Subspecies: *Rutpela (Rutpela) maculata irmasanica* Sama, 1996
Distribution: Anatolia (Antalya) (Fig. 2)
Remarks: Likely not a distinct subspecies, representing only an infrataxonomic color aberration. Requires precise molecular investigation.

Subspecies: *Rutpela (Rutpela) maculata manca* (Schaufuss, 1863)
Distribution: Southwestern Europe, including the Iberian Peninsula; southern, central, and western France; the British Isles; Maritime Alps; Corsica and Sardinia; central and southern Italy; Sicily (Fig. 2).

Subspecies *Rutpela maculata orientalis* **ssp. nov.**
Holotype (Fig. 3): Male (Guzeripl, Adygea, Caucasus, 17.VI.1958, ex coll. I. Zahajkevych; deposited in PUIF, Ivano-Frankivsk, Ukraine), 1.7 mm. Body elongated, tapered posteriorly, black. Head elongate; eyes strongly convex; occipital spot and mouthparts yellow-orange, except terminal segments. Antennae black with very narrow pale rings at base of antennomeres 4–11. Pronotum subcylindrical, lateral tubercles broadly rounded. Elytra yellow with four fasciae, two anterior incomplete. Metathorax with two longitudinal lamellar keels on disc. Procoxae with small plate-like projections. Fore- and midlegs yellow, tibial apices and tarsomeres darker (dirty-orange/light-

brown). Hindlegs with deep tibial notch, armed with small teeth, dark brown-black except light basal femur; all coxae and trochanters black.

Figure 3. Holotype of *Rutpela maculata orientalis* **ssp. nov.**

Paratype: Female (Guzeripl, Adygea, Caucasus, 17.VI.1958, in coll. I. Zahajkevych; deposited in SMNH, Lviv, Ukraine), 2.1 mm. Similar to holotype, body broader and slightly convex. Antennae with wide pale rings on bases of antennomeres 3–11. Abdomen with pale basal sternites. Legs yellow except tibial apices, tarsomeres, and dorsal half of hind femur; coxae and trochanters black.

Variation: Males occasionally exhibit entirely black antennomeres without pale rings. Sometimes hindlegs are slightly lighter, ranging from dark brown to rusty-brown. In females, hind tibiae may occasionally be darker. Both sexes frequently show color aberrations of the elytra, differing in number and shape of fasciae and spots.

Type locality: Mountains south of Guzeripl, Adygea, Caucasus.

DNA barcode diagnosis: C–82; C–104; G–196; C–508; C–646.

Etymology: Latin *orientalis* – "eastern", referring to the eastern part of the *R. maculata* range.

Distribution: Crimean Mountains, Caucasus-Caspian region, Anatolia (primarily eastern and central parts) (Fig. 2).

Remarks: L. Heyrovský (1936) described *Strangalia maculata a. veselyi n.* from the Caucasus (Svaneti, Georgia) – a rare aberration distinguished by an interrupted third elytral fascia. However, this aberration does not correspond to subspecific rank under Art. 45.6.2 of the Code, and thus the name is unavailable for use.

4. CONCLUSIONS

In summary, our study using molecular phylogenetic methods resolved the long-standing issue of the intraspecific classification of *Rutpela maculata*, including the geographic boundaries of its subtaxa. Furthermore, we demonstrated, through a concrete example, the high effectiveness of molecular approaches in addressing multi-level taxonomic, evolutionary, ecological, and biogeographic questions.

Acknowledgments. We would like to express our sincere gratitude to Dr. Taras Yanytskyi, Director of the State Museum of Natural History of the NAS of Ukraine (Lviv, Ukraine), for providing free and unlimited access to the collections and laboratories. We are also very grateful to Dr. Kateryna Hushtan, Entomological collection curator of the State Museum of Natural History of the NAS of Ukraine (Lviv, Ukraine), for her comprehensive assistance during the collections study.

Author contributions. Conceptualization: AZ. Methodology, data collection, figures, tables, and referencing: AZ, OZ. Writing – original draft preparation: AZ, OZ. Writing – review and editing: AZ.

Funding.

A.Z. the study was conducted as part of the ongoing scientific research project titled "Molecular phylogeny and systematics of living organisms" (state registration number 0121U109305) at Vasyl Stefanyk Carpathian National University.

O.Z. have also received support through the EURIZON project, which is funded by the European Union under grant agreement No.871072, and laboratory work was possible due to the support of the Academic Sanctuaries Fund created by XTX Markets. The sequences were obtained as a part of training activities of Biodiversity Genomics Europe (Grant no.101059492), funded by Horizon Europe under the Biodiversity, Circular Economy and Environment call (REA.B.3); co-funded by the Swiss State Secretariat for Education, Research and Innovation (SERI) under contract numbers 22.00173 and 24.00054; and by the UK Research and Innovation (UKRI) under the Department for Business, Energy and Industrial Strategy's Horizon Europe Guarantee Scheme.

Data availability. Sequence data presented in this paper will be publicly available at GenBank after December, 1, 2025 (accession numbers: PV658009; PX418918; PX418919; PX418920; PX418921).

Declarations

Conflict of interest. The authors declare that the research was conducted in the absence of any commercial or other relationships that could be construed as a potential conflict of interest.

Research involving human participants and/or animals. This study did not involve any experiments on humans or animals. All data were obtained from studies that did not require direct involvement of human participants or experimental use of animals.

REFERENCES

Anisimova M & Gascuel O (2006) Approximate likelihood ratio test for branches: A fast, accurate and powerful alternative. Systematic Biology, 55(4):539–552. https://doi.org/10.1080/10635150600755453

Barek H, Sugumaran M, Ito S, Wakamatsu K (2017) Insect cuticular melanins are distinctly different from those of mammalian epidermal melanins. Pigment Cell Melanoma Res 31:384–392. https://doi.org/10.1111/pcmr.12672

Danilevsky ML (2015) Longicorn beetles (Coleoptera, Cerambycoidea) of Russia and adjacent countries. Part 1. HSC.

Gascuel O (1997) BIONJ: An improved version of the NJ algorithm based on a simple model of sequence data. Molecular Biology and Evolution, 14(7):685–695. https://doi.org/10.1093/oxfordjournals.molbev.a025808

Gouy M, Tannier E, Comte N, & Parsons DP (2021) Seaview Version 5: A multiplatform software for multiple sequence alignment, molecular phylogenetic analyses, and tree reconciliation. Methods in Molecular Biology, 2231:241–260. https://doi.org/10.1007/978-1-0716-1036-7_15

Guindon S, Dufayard JF, Lefort V, Anisimova M, Hordijk W, & Gascuel O (2010) New algorithms and methods to estimate maximum-likelihood phylogenies: Assessing the performance of PhyML 3.0. Systematic Biology, 59(3):307–321. https://doi.org/10.1093/sysbio/syq010

Haque MT, Khan MK, Herberstein ME (2024) Current evidence of climate-driven colour change in insects and its impact on sexual signals. Ecol Evol 14: e11623. https://doi.org/10.1002/ece3.11623

Heyrovský L (1936) Dritter Beitrag zur Kenntnis der Gruppe Lepturini (Col., Ceramb.). Časopis České Společnosti Entomologické, Praha 33:52–57

Korlević P, McAlister E, Mayho M, Makunin A, Flicek P, & Lawniczak MKN (2021) A minimally morphologically destructive approach for DNA retrieval and whole-genome shotgun sequencing of pinned historic Dipteran vector species. Genome Biology and Evolution, 13(10). https://doi.org/10.1093/gbe/evab226

Kutama DM, Minnaar IA, Starostová Z, Clusella-Trullas S (2024) Developmental plasticity of melanisation in a beetle reveals sex-specific responses and performance costs. Ecol Entomol 49:624–634. https://doi.org/10.1111/een.13333

Löbl I, Smetana A (eds) (2010) Catalogue of Palaearctic Coleoptera, Vol. 6. Chrysomeloidea. Apollo Books, Stenstrup

Makunin A, Korlević P, Park N, Goodwin S, Waterhouse RM, von Wyschetzki K, Jacob CG, Davies R, Kwiatkowski D, St. Laurent B, Ayala D, & Lawniczak MKN (2022) A targeted amplicon sequencing panel to simultaneously identify mosquito species and *Plasmodium* presence across the entire *Anopheles* genus. Molecular Ecology Resources, 22(1):28–44. https://doi.org/10.1111/1755-0998.13436

Mulsant E (1839) Histoire Naturelle des Coléoptères de France. Longicornes. Maison, Paris

Özdikmen H, Mercan N, Cihan N, Özbek H (2012) Subspecific status of *Rutpela maculata* (Poda, 1761) (Coleoptera: Cerambycidae: Lepturinae). Munis Entomol Zool 7:516–522

Özdikmen H (2021) A discussion on taxonomic position of *Rutpela maculata manca* (Schaufuss, 1863) (Cerambycidae: Lepturinae: Lepturini). Munis Entomol Zool 16:411–418

Pic M (1933) Notes diverses, nouveautés (Suite.). L'Échange, Revue Linnéenne 49:1–2

Pic M (1937) Notes diverses, nouveautés (Suite.). L'Échange, Revue Linnéenne 53:13–15

Pic M (1945) Coléoptères du globe (suite). L'Échange, Revue Linnéenne 61:13–16

Poda N (1761) Insecta Musei Græcensis, quæ in ordines, genera et species Juxta Systema Naturæ Caroli Linnæi digessit Nicolaus Poda. Widmanstad, Vienna.

Podaný Č (1963) Nouvelles formes de Cérambycides (Col.). Bull Soc Entomol Mulhouse (Jan–Feb 1963):9–10

Rapuzzi P, Sama G (2006) Cerambycidae nuovi o interessanti per la fauna di Sicilia (Insecta: Coleoptera: Cerambycidae). Quad Studi Nat Romagna 23:157–172

Sama G (1996) Contribution à la connaissance des Longicornes de Grèce et d'Asie Mineure (Coleoptera, Cerambycidae) Biocosme Mésogéen, Nice 12(4):101–116

Semaniuk DV, Zamoroka AM (2020) Preliminary phylogenetic analysis of Lepturini (Insecta: Coleoptera: Cerambycidae). In: XVI International scientific conference for students and PhD students "Youth and Progress of Biology", Lviv, p. 121

Srivathsan A, Lee L, Katoh K, Hartop E, Kutty SN, Wong J, Yeo D, & Meier R (2021) ONTbarcoder and MinION barcodes aid biodiversity discovery and identification by everyone, for everyone. BMC Biology, 19(1). https://doi.org/10.1186/s12915-021-01141-x

Srivathsan A, Feng V, Suárez D, Emerson B, & Meier R (2024) ONTbarcoder 2.0: Rapid species discovery and identification with real-time barcoding facilitated by Oxford Nanopore R10.4. Cladistics, 40(2):192–203. https://doi.org/10.1111/cla.12566

Sivell O, Sivell D, Barclay MVL, Crowley LM (2023) The genome sequence of a longhorn beetle, *Rutpela maculata* (Poda, 1769). Wellcome Open Res 8:579. https://doi.org/10.12688/wellcomeopenres.20500.1

Sugumaran M, Barek H (2016) Critical analysis of the melanogenic pathway in insects and higher animals. Int J Mol Sci 17:1753. https://doi.org/10.3390/ijms17101753

Vitali F (2018) Atlas of the Insects of the Grand-Duchy of Luxembourg: Coleoptera, Cerambycidae. Ferrantia 79, Musée national d'histoire naturelle, Luxembourg

Zamoroka AM (2022a) The longhorn beetles (Coleoptera: Cerambycidae) of Ukraine: Results of two centuries of research. Biosystem Diversity, 30:46–74. https://doi.org/10.15421/012206

Zamoroka AM (2022b) Molecular revision of Rhagiini sensu lato (Coleoptera, Cerambycidae): Paraphyly, intricate evolution and novel taxonomy. Biosystem Diversity, 30:295–309. https://doi.org/10.15421/012232

Zamoroka AM, Trócoli S, Shparyk VYu, Semaniuk DV (2022) Polyphyly of the genus *Stenurella* (Coleoptera, Cerambycidae): Consensus of morphological and molecular data. Biosystem Diversity, 30:119–136. https://doi.org/10.15421/012212

Zamoroka A, Zinenko O (2024) Taxonomic position of *Tetrops peterkai* Skořepa, 2020 (Coleoptera: Cerambycidae) and its cryptic distribution. Journal of Vasyl Stefanyk Precarpathian National University. Biology, 11:6–19. https://doi.org/10.15330/jpnubio.11.6-19

Zamoroka A (2025a) Integrative Approaches for Precise Identification and Range Delimitation of the Three Most Common European Leiopus species (Coleoptera, Cerambycidae). Zoodiversity, 59(1): 45–68. http://dx.doi.org/10.15407/zoo2025.01.045

Zamoroka A (2025b) When Morphology Meets Molecules: Barcoding Confirms an Ancient Separation of Phytoecia tigrina subspecies (Coleoptera, Cerambycidae). Zoodiversity, 59(5): 477–492. https://doi.org/10.15407/zoo2025.05.477

Andrew M. Zamoroka, PhD, Associate Professor
Laboratory of Animal Phylogeny and Evolution, Department of Biology and Ecology, Vasyl Stefanyk Carpathian National University, Shevchenko str., 57, Ivano-Frankivsk, Ukraine, 76018
E-mail: andrew.zamoroka@pnu.edu.ua, andrii.zamoroka@cnu.edu.ua
ORCID ID: https://orcid.org/0000-0001-5692-7997

Oleksandr I. Zinenko, PhD, Leading Researcher, Associate Professor
The Museum of Nature, and Department of Zoology and Animal Ecology, School of Biology, V. N. Karazin Kharkiv National University, Svobody sq. 4, Kharkiv, 61022, Ukraine
E-mail: oleksandrzinenko@karazin.ua
ORCID ID: https://orcid.org/0000-0001-5228-9940

Заморока А.М., Зіненко О.І. Перехресна молекулярна валідація внутрішньовидової структури *Rutpela maculata* (Insecta: Coleoptera: Cerambycidae). *Журнал Прикарпатського національного університету імені Василя Стефаника. Біологія*, 12: 46-59.

Анотація

Rutpela (Rutpela) maculata (Poda, 1761) є одним із найпоширеніших і масових скрипунових жуків у Європі, з ареалом від Атлантичного узбережжя на заході до Південного Уралу на сході. Впродовж останніх десятиліть внутрішньовидова таксономія *R. maculata* за морфологічними ознаками була предметом дискусій, і консенсус щодо її організації досі відсутній. У цьому дослідженні проведено філогенетичний аналіз внутрішньовидової структури *R. maculata* на основі нових ДНК-баркодів із Хорватії, Італії, Словенії, Іспанії та України, а також доступних у публічних базах даних (GenBank, BOLD Systems, CaBOL). Результати свідчать про наявність трьох чітко відокремлених гаплогруп (*weRM*, *ceRM*, *esRM*), кожна з яких асоційована з низкою морфологічних ознак, особливо меланізацією кінцівок у самців. Меланістичні форми гаплогрупи *weRM* у Південно-Західній Європі та гаплогрупи *esRM* у

Кавказько-Анатолійському регіоні виникли ізольовано і незалежно, тоді як гаплогрупа *ceRM* має значне поширення в Європі – від Фінляндії та Норвегії до Італії та Хорватії. Дві гаплогрупи відповідають відомим підвидам – *R. m. maculata* (*ceRM*) та *R. m. manca* (*weRM*). Третя гаплогрупа *esRM*, яку раніше розглядали як частину *R. m. manca*, виявилася окремою еволюційною лінією, спорідненою з *ceRM*, і формально запропонована як новий підвид *Rutpela maculata orientalis* **ssp. nov**. Генетичні відстані, відмінності в COI-послідовностях, морфологічні та географічні відмінності підтверджують цю таксономічну ревізію. Дослідження демонструє ефективність молекулярних філогенетичних підходів для вирішення давніх питань внутрішньовидової класифікації та визначення ареалів підвидів *R. maculata*.

Ключові слова: скрипунові жуки, молекулярна філогенія, молекулярна філогеографія, систематика, ПЛР, ДНК баркодинг